Ovodok, E.; Maltanava, H.; Poznyak, S.; Ivanovskaya, M.; Kudlash, A.; Scharnagl, N.; Tedim, J.:
Sol-gel template synthesis of mesoporous carbon-doped TiO2 with photocatalytic activity under visible light.
In: Materials Today: Proceedings. Vol. 5 (2018) 9-2, 17422 - 17930.
First published online by Elsevier: August 29, 2018

DOI: 10.1016/j.matpr.2018.06.044
https://dx.doi.org/10.1016/j.matpr.2018.06.044

ANM2017

Sol-gel template synthesis of mesoporous carbon-doped TiO_2 with photocatalytic activity under visible light

Evgeni Ovodok[a], Hanna Maltanava[a]*, Sergey Poznyak[a], Maria Ivanovskaya[a], Alexander Kudlash[b], Nico Scharnagl[c], Joao Tedim[d]

[a]*Research Institute for Physical Chemical Problems, Belarusian State University, Leningradskaya str. 14, 220030 Minsk, Belarus*
[b]*Faculty of Chemistry, Belarusian State University, Nezavisimosti ave. 4, 220030 Minsk, Belarus*
[c]*Helmholtz-Zentrum Geesthacht, Centre for Materials and Coastal Research GmbH, Max-Planck-Straße 1, 21502 Geesthacht, Germany*
[d]*Department of Materials and Ceramics Engineering, CICECO-Aveiro Institute of Materials, The University of Aveiro, Campus Universitário de Santiago, 3810-193 Aveiro, Portugal*

Abstract

Mesoporous TiO_2 powders with an anatase framework were synthesized through surfactant-assisted template method. The concentrated titania sol (7-8 wt.%) prepared from $TiCl_4$ as a precursor was used in this synthesis. The soluble triblock copolymer Pluronic F127 was employed as a structure-directing agent and a carbon precursor to fabricate the carbon-doped mesoporous titania. The synthesized powders were characterized by XRD, HRTEM, Raman spectroscopy, UV-Vis reflectance spectroscopy, N_2 adsorption/desorption and TG/DSC methods. The mesoporous titania annealed at 350° C was shown to have a high specific surface area up to 192 m^2/g and a narrow pore size distribution. After annealing, carbon species in graphitic form were detected in the template-prepared TiO_2 samples using Raman spectroscopy measurements. The photocatalytic performance of the samples was characterized in the process of Rhodamine B decomposition under visible light irradiation. The enhanced visible light photocatalytic efficiency of the template-prepared TiO_2 powders as compared with that of Degussa P25 can be attributed to the associated effects of high specific surface area, pure anatase crystalline structure and carbon doping.

Keywords: Titanium dioxide; Mesoporous materials; Sol gel; Carbon-doped; Photocatalysis

* Corresponding author. Tel.: +3-751-720-953-02.
E-mail address: annamaltanova@gmail.com

Selection and/or Peer-review under responsibility of ANM2017.

Selection and/or Peer-review under responsibility of ANM2017.

1. Introduction

Mesoporous oxides have attracted much attention in different fields (adsorbents, sensors, electrode materials for energy conversion and storage devices, etc.) owing to their exceptional properties including ultrahigh surface area, large pore volume, tunable pore size and shape [1]. Among various oxides, titania is considered as a very important material due to many promising applications ranging from photovoltaics and photocatalysis to electrochromics and sensors [2]. Mesoporous titania was first synthesized by Antonelli and Ying through a modified sol-gel process using a phosphate surfactant as template [3]. Later, a variety of methods has been proposed to improve the specific surface area, crystallinity and pore size of mesoporous TiO_2 [4–7]. In particular, triblock copolymers belonging to the group of polyoxyethylene–polyoxypropylene–polyoxyethylene surfactants have been successfully used as templates for the synthesis [8].

Unfortunately, titania, as photocatalyst, exhibits some intrinsic drawbacks, such as limited visible light absorption due to wide band gap, which hinders its efficiency and more widespread applications. Many efforts have been made to overcome this limitation and to achieve the utilization of visible light for TiO_2 material. Three general strategies have been explored for this purpose; two of them consist of doping of TiO_2. Doping with both transition metal ions [9] and non-metal elements [10] such as N, P, F, B, C and S, can extend the photoresponse of TiO_2 into visible region. Generally, doping with non-metal elements is claimed to produce more stable photocatalysts. In this connection, it is of interest to search for new methods of simultaneous synthesis of mesoporous and doped TiO_2 with sensitivity to visible light.

In the present work, we report a method for preparing carbon-doped mesoporous titania with a high surface area. In this synthesis Pluronic F127 (PL) was used simultaneously as a structure-directing agent and as a carbon source. The resultant TiO_2 samples were characterized by XRD, HRTEM, confocal Raman spectroscopy, N_2 adsorption/desorption and TG/DSC methods. In addition, photocatalytic activity of the samples was evaluated in the photodegradation of Rhodamine B (RhB) under visible light irradiation and compared with a commercial Degussa P25 TiO_2.

2. Experimental

2.1. Titania powder preparation

TiO_2 concentrated sol was prepared by the following method. 15 mL of distilled $TiCl_4$ were added dropwise to 53 mL of 0.65 M HCl aqueous solution (cooled to 0 °C) under vigorous stirring in ice-water bath, giving a clear yellowish solution. If turbidity of the solution appears, it should be filtered on a glass filter. The resultant transparent solution was diluted with distilled water to 250 mL and then titrated slowly by a 12 % aqueous ammonia solution (appr. 1 drop per 2 s) under continuous stirring at 0 °C. During the titration, it is necessary to check periodically the pH of solution. Upon reaching pH 4–5 the suspension becomes very viscous. Then, the suspension was centrifuged at a rotation speed of 2500 rpm. After discarding the supernatant, the precipitate was washed thoroughly with distilled water until the washings were chloride-free. After adding 0.9 mL of concentrated HNO_3 (65 wt. %) as a sol stabilizer, the precipitate was stirred to give a movable suspension. Then, the suspension was ultrasonically (frequency – 22 kHz) treated with an ultrasonic horn placed into a beaker with the suspension to obtain a transparent opalescent sol. The prepared sol contains 7–8 wt. % of TiO_2 and is stable for several months at room temperature.

In order to produce TiO_2 powders with mesoporous structure a block copolymer Pluronic F127 (designated hereafter as PL) was used as a template. This copolymer was added to the TiO_2 sol with different TiO_2:copolymer ratios – 4:1, 2:1 and 1:1 (by weight). To prevent a possible decrease of the titania powder specific surface area, lyophilization at -77 °C was applied for dehydration of the TiO_2 sol. Finally, the TiO_2 powder was annealed at different temperatures in air for 1 h and then in oxygen atmosphere for 1 h (the heating rate of 10 °C/min).

2.2. Characterization

The XRD analysis of the TiO_2 powders was performed on a PANalytical X'Pert PRO MRD (Multi-Purpose Research Diffractometer, Holland) using CuK_α-radiation. The crystallite size was estimated by applying the Scherrer equation to the FWHM of the (101) peak of anatase, with LaB_6 as a standard for the instrumental line broadening.

The surface area and porous structure of the samples were characterized on a Micromeritics ASAP 2020 system using nitrogen at 77 K.

The TG/DSC analysis of the titania powders was performed on a NETZSCH STA 449C instrument over the temperature range from 30 to 800 °C in air ambient.

High-resolution transmission electron microscopy (HRTEM) was carried out using a Philips CM 300 UT microscope operating at 300 kV. TEM samples were prepared from the annealed xerogels dispersed in ethanol under sonification. The dispersion was dropped onto a carbon-coated copper grid and the solvent was evaporated immediately.

Fourier transform infrared (FTIR) spectra were measured on an AVATAR-330 (Thermo Nicolet) spectrometer supplied with a diffuse reflectance accessory in the wavenumber range from 400 to 4000 cm^{-1}. Raman spectra were registered at room temperature using a confocal Nanofinder HE (LOTIS TII, Belarus – Japan) spectrometer. Solid-state laser emitting at 532 nm (intensity – 2 mW) was used for excitation of the samples.

Photocatalytic properties of the TiO_2 samples were investigated in the process of Rhodamine B decomposition in an aqueous solution under visible irradiation. In each experiment, 100 mg of TiO_2 catalyst was dispersed in 100 mL of 0.02 mM RhB solution in a quartz cylindrical reactor and stirred in the dark for 2 h to establish adsorption-desorption equilibrium. A halogen lamp (50 W) equipped with reflector and UV and infrared filters was used as the visible light source. The suspension was slightly stirred using a magnetic stirrer during the irradiation. 1 mL of the suspension was withdrawn after defined time intervals of irradiation. The suspension was centrifuged at 10000 rpm and the clear supernatant was analyzed by UV–vis spectroscopy (Shimadzu UV- 2550 spectrophotometer).

3. Results and discussion

3.1. TG/DSC measurements

To determine the adequate temperature range for thermal treatment of the TiO_2 powders, TG/DSC analysis of the dried xerogels was carried out. The thermogravimetric study of the samples showed a continuous weight loss from room temperature to approximately 450 °C. Three main steps can be found during these thermochemical transformations (Fig. 1).

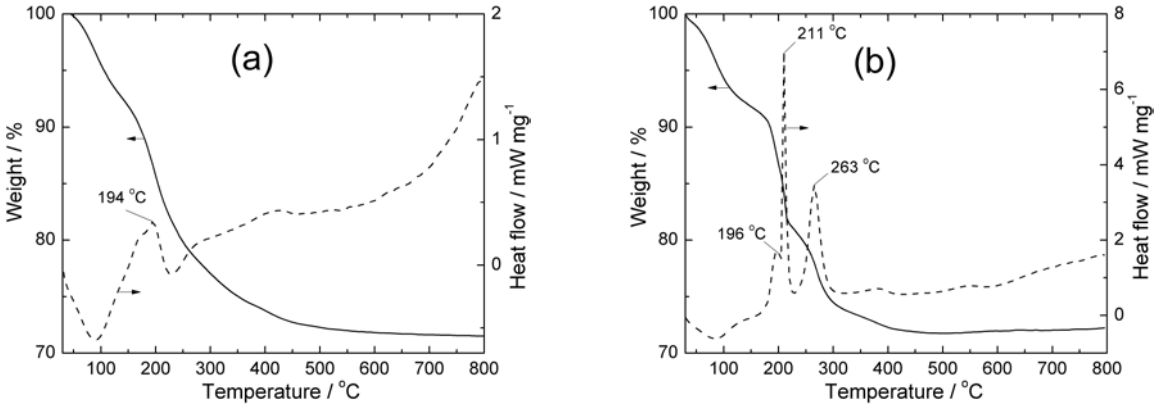

Fig. 1. TG/DSC curves for sol-gel-derived TiO_2 xerogel prepared without (a) and with Pluronic (b).

An initial weight loss in the temperature range from 30 to *ca*. 150 °**C** is accompanied by an endothermic effect and can be related to withdrawal of physically adsorbed water and unbound stabilizing acid from the powder. For template-free sample, a subsequent sharp decrease in the weight observed in the range from 150 to 250 °**C** seems to be associated with removal of the structural water. Crystallization of the amorphous phase also starts in this temperature interval. These processes are accompanied by the exothermic effect being superimposed on the endothermic one (Fig. 1a). Above 250 °**C**, the weight loss becomes smoother and then is practically negligible. For TiO_2 xerogel containing Pluronic as a structure-directing agent, between 180 and 290 °C there are three sharp mass losses (ca. 15 %) related to decomposition of the Pluronic template along with dehydration of the $TiO_2 \cdot nH_2O$ (Fig. 1b). Very rapid mass loss at 211 °**C** accompanied by an extremely fast heat evolution can be associated with the explosive autocatalytic process of thermal-oxidative degradation of Pluronic, proceeding with participation of products of nitric acid decomposition. Some residual organic matter and tightly coupled hydroxyl groups are removed at temperatures between 300 and 450 °C.

Since annealing at temperatures above 350 °C leads to an appreciable decrease in the surface area of the powders and to degradation of their mesoporous structure, most of the experiments were performed on the samples heated at 350 °C.

3.2. XRD analysis

X-ray diffraction analysis showed that the sol-gel derived TiO_2 powders annealed at temperatures from 200 to 450 °C consist of anatase phase only. Anatase-to-rutile transformation begins at *ca*. 500 °C and is completed in the temperature interval from 700 to 750 °C. The mean size of anatase crystallites calculated from the half-width of the (101) diffraction peak is about 5 nm for the samples heated at 200 °C and grows up to 7–8 nm after annealing at 400 °C. Pluronic addition to the sol does not influence the obtained diffraction patterns of the annealed xerogels appreciably (Fig. 2), but the mean size of crystallites for the samples heated at 350 °C decreases from 6.3 till 4.9 nm with increasing the PL:TiO_2 ratio in sol from 0 to 1:2 (Table 1).

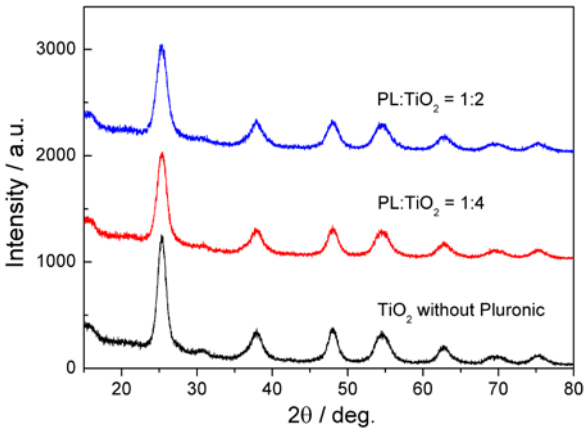

Fig. 2. X-ray diffractograms of sol-gel-derived TiO_2 xerogels without and with addition of Pluronic annealed at 350ºC.

3.3. Transmission electron microscopy

Figure 3 presents high-resolution TEM image of the TiO_2 xerogel annealed at 350°C. The image shows that the powder consists of a large number of tiny nanocrystals that are closely interconnected with each other. The crystallites have a mean size consistent with that calculated from the XRD data. The HRTEM patterns demonstrate lattice fringes for most particles, indicating nanocrystalline anatase.

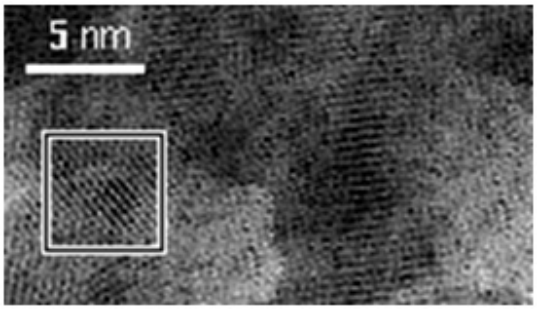

Fig. 3. High resolution TEM image of sol-gel-derived TiO_2 xerogel annealed at 350ºC.

3.4. BET measurements

To gain a better understanding of the porous structure of the sol-gel derived TiO_2 powders, the N_2 adsorption–desorption isotherm and BJH pore size distribution were collected, as shown in Fig. 4.

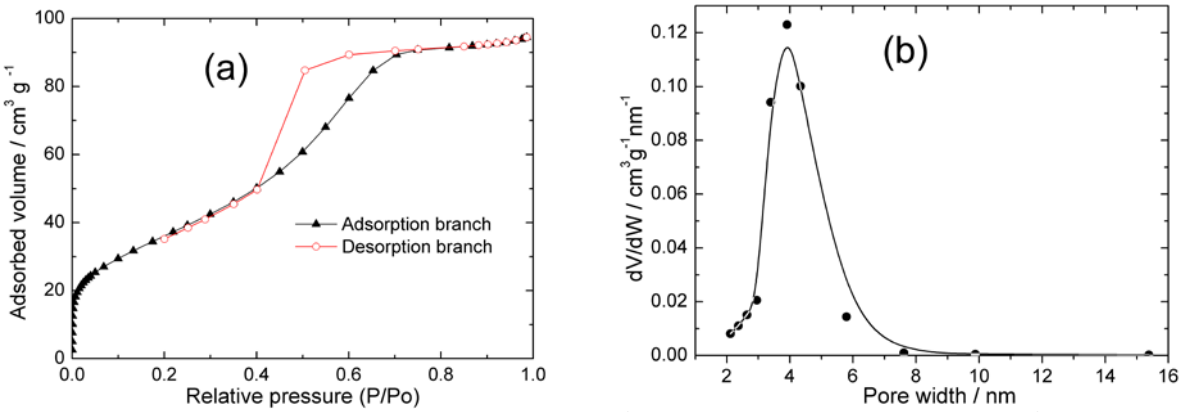

Fig. 4. N_2 adsorption–desorption isotherm (a) and pore size distribution (b) for sol-gel-derived TiO_2 xerogel with addition of Pluronic (PL:TiO_2 = 1:2) annealed at 350ºC.

All samples exhibit a type IV isotherm with a H2 hysteresis loop at a relative pressure (P/P_0) of 0.4–0.7 (Fig. 4a), which is characteristic of mesoporous solids [11]. The BJH pore size distribution curves obtained from the adsorption–desorption isotherms indicate that the TiO_2 samples contain mesopores with a diameter in the range of 3–5 nm (Fig. 4b). The specific surface area, calculated by the multi-point Brunauer-Emmett-Teller (BET) method, is 108 $m^2 g^{-1}$ for the sample prepared without template and increases up to 192 $m^2 g^{-1}$ for the sample with a PL:TiO_2 ratio of 1:2. Structural characteristics of different sol-gel-derived TiO_2 samples are compared in Table 1.

Table 1. Structural characteristics obtained from XRD and BET measurements for sol-gel-derived TiO_2 powders annealed at 350ºC.

Sample	Crystallite size* (nm)	Average pore diameter (nm)	Total pore volume ($cm^3 g^{-1}$)	BET surface area ($m^2 g^{-1}$)
TiO_2	6.3	3.3	0.109	108
PL:TiO_2=1:4	5.7	3.6	0.146	134
PL:TiO_2=1:2	4.9	3.9	0.232	192

*Average crystallite size calculated from X-ray diffractograms.

3.5. UV-Vis reflectance spectroscopy

We found that the color of the annealed mesoporous titania powders synthesized without template and with Pluronic was different. While the template-free TiO_2 sample was white, the samples prepared with Pluronic showed color ranging from yellow to brown. Fig. 5 presents the UV–Vis diffuse reflectance spectra of the titania samples under study.

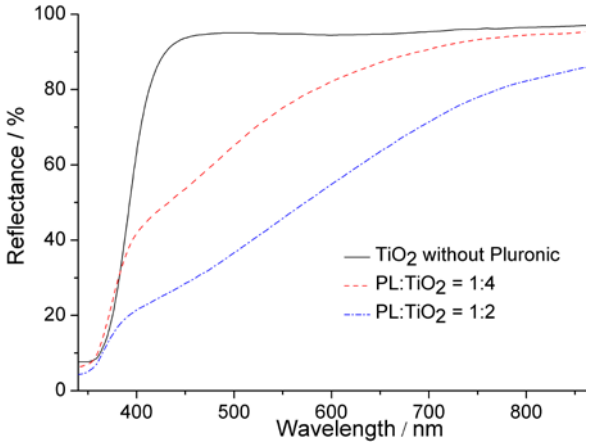

Fig. 5. Diffuse reflectance spectra of sol-gel-derived TiO_2 xerogels without and with addition of Pluronic annealed at 350°C.

It is clearly seen from Fig. 5 that the powders synthesized with Pluronic demonstrate increased absorption in the wavelength range $\lambda > 450$ nm and the absorption tails extend to 850 nm and more. The absorption in the visible light region grows with increasing the PL:TiO_2 ratio. We suspected that carbon species appeared in the process of thermal-oxidative degradation of Pluronic are responsible for the visible light absorption. To support this suggestion, Raman spectroscopy measurements were taken.

3.6. Raman spectroscopy

Raman spectroscopy is an effective tool to investigate and characterize different carbon materials. Figure 6 shows the Raman spectra of the template-free TiO_2 powder and the powder synthesized with Pluronic.

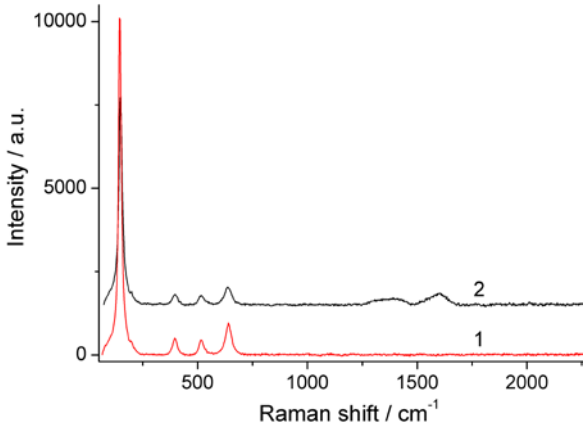

Fig. 6. Raman spectra of sol-gel-derived TiO_2 powders synthesized without (1) and with Pluronic (2).

It can be seen that both samples exhibit the distinct Raman-active modes of the anatase phase at 146, 397, 517 and 640 cm^{-1}, confirming the phase composition determined by XRD. The presence of carbon in the template-synthesized

TiO_2 powder is evidenced by the Raman modes in high energy region (1300–1600 cm^{-1}) as shown in Fig. 6 (curve 2). The well-documented *D*- and *G*-bands, generally observed for graphitic carbon [12], can be observed at ~1390 and ~1600 cm^{-1}, respectively. These results indicate that the carbon species are present in graphitic form (C–C) in the TiO_2 samples prepared with Pluronic even after their annealing at 350 °C in oxygen atmosphere.

3.7. Photocatalytic degradation of Rhodamine B aqueous solutions under visible irradiation.

The photocatalytic activity of the synthesized mesoporous TiO_2 nanopowders was evaluated by the degradation of RhB aqueous solution under visible irradiation. For comparison, the activity of commercial nonporous photocatalyst Degussa P25 was also measured under identical conditions. A control experiment was also carried out with TiO_2-free RhB solution. In this case no appreciable photobleaching was observed during 4 h of irradiation. Initial solution of RhB before photodegradation shows a major absorption band peaked at 554 nm. Under visible light irradiation in the presence of the TiO_2 particles, the spectrum of this solution is changed: the peak is shifted to shorter wavelengths and the maximum absorbance decreases. The shift of the absorbance peak deceases at *ca.* 498 nm and then only the peak intensity continues to drop (Fig. 7).

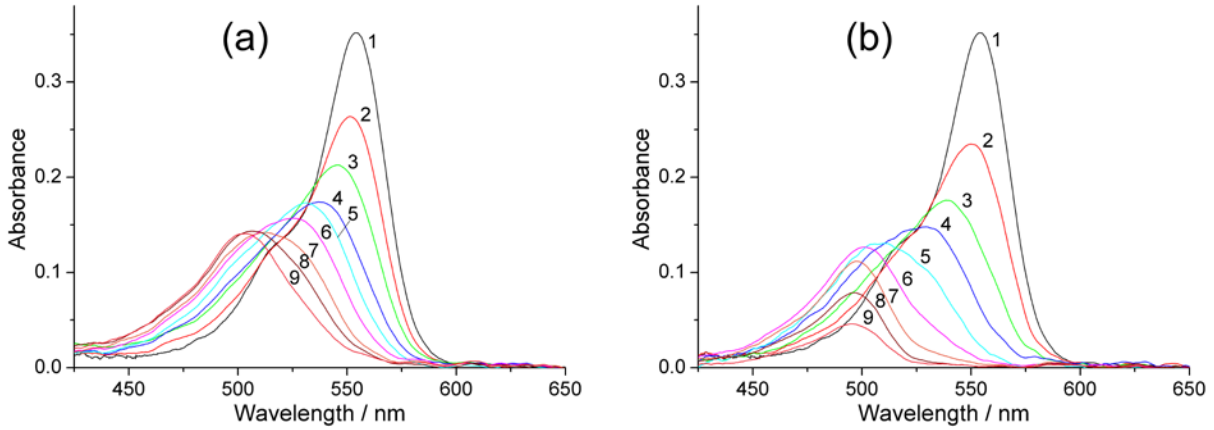

Fig. 7. Change in the absorption spectrum of Rhodamine B solutions, loaded with sol-gel-derived TiO_2 particles synthesized without (a) and with Pluronic (PL:TiO_2 ratio = 1:2) (b), with time of visible light illumination: 1 – 0; 2 – 30; 3 – 60; 4 – 90; 5 – 120; 6 – 150; 7 – 180; 8 – 210 and 9 – 240 min.

This transformation of the spectrum is in accordance with previously reported observations and can be explained by a stepwise de-ethylation of Rhodamine B molecules which leads to the fully de-ethylated rhodamine species having an absorbance peak at 498 nm [13]. Visible light irradiation for longer times results in further decomposition of the de-ethylated rhodamine intermediates with cleavage of the RhB chromophore ring structure as indicated by decrease in the absorbance at 498 nm (Fig. 7b). It is important to note that this photocatalytic reaction proceeds mainly by light absorption of adsorbed dye molecules and to a lesser extent by excitation of TiO_2. The titania acts only as a mediator for transferring electrons from the excited dye to the TiO_2 conduction band. Then, the injected electrons are scavenged by molecular oxygen producing superoxide radical $O_2^{\bullet-}$ and hydrogen peroxide radical $^{\bullet}OOH$. The subsequent radical reactions lead to the degradation of the RhB.

The temporal evolution of the maximum absorbance of the solution during Rhodamine B degradation mediated by different TiO_2 particles is shown in Figure 8.

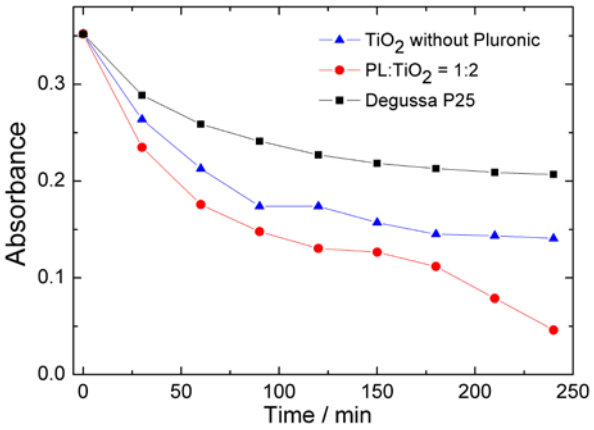

Fig. 8. Temporal evolution of the maximum absorbance (major absorption band in the visible region) of Rhodamine B solutions in the presence of different sol-gel-derived TiO_2 particles and Degussa P25 during visible light irradiation.

The results obtained clearly demonstrate the good performance of the mesoporous samples. The maximum activity is observed for the template-prepared sample with a PL:TiO_2 ratio of 1:2. Moreover, all of the synthesized materials show better activity than Degussa P25 (Fig. 8).

Several reasons can account for the enhanced visible-light activity of the mesoporous TiO_2 powders. First, these samples with high surface area can provide more active sites and adsorb more reactive species. Second, the carbon doping of TiO_2 may lead to the band gap narrowing [14]. As a result, C-doped TiO_2 can absorb more visible light. In addition, carbon species detected in the TiO_2 samples prepared with Pluronic may act as a visible-light sensitizer for the TiO_2 as a photocatalyst [15].

4. Conclusion

Carbon-doped mesoporous TiO_2 powders have been successfully prepared from concentrated titania sols using Pluronic F127 as a structure-directing agent and a carbon-doping source. The samples treated at an optimum temperature of 350° C demonstrate nanocrystalline anatase structure and high surface area with abundance of reaction sites. Explosive autocatalytic process of thermal-oxidative degradation of Pluronic may be responsible for these structural characteristics. The presence of carbon species in graphitic form in the TiO_2 samples prepared with Pluronic has been proved by Raman spectroscopy. The synthesized TiO_2 powders were found to be photocatalytically active in degradation of Rhodamine B in aqueous solutions under visible light irradiation. The most photocatalytically active sample under illumination of visible light is the template-prepared powder with a Pluronic:TiO_2 ratio of 1:2.

Acknowledgements

We acknowledge funding from SMARCOAT project. This project has received funding from the European Union's Horizon 2020 research and innovation programme under the Marie Skłodowska-Curie grant agreement No 645662. This work was also developed in the scope of the project CICECO – Aveiro Institute of Materials, POCI-01-0145-FEDER-007679 (Ref. FCT UID/CTM/50011/2013), financed by national funds through the FCT/MEC and when applicable co-financed by FEDER under the PT2020 Partnership Agreement. JT thanks FCT for the research grant IF/00347/2013.

References

[1] M. E. Davis, Nature 417 (2002) 813–821.
[2] X. Chen, S. S. Mao, Chem. Rev. 107 (2007) 2891–2959.
[3] D. M. Antonelli, J. Y. Ying, Angew. Chem. Int. Ed. Engl. 34 (1995) 2014–2017.
[4] P. Yang, D. Zhao, D. I. Margolese, B. F. Chmelka, G. D. Stucky, Nature 396 (1998) 152–155.

[5] J. Zheng, J. Pang, K. Qiu, Y. Wei, J. Mater. Chem. 11 (2001) 3367–3372.
[6] D. Grosso, G. J. de A. A. Soler-Illia, E.L. Crepaldi, F. Cagnol, C. Sinturel, A. Bourgeois, A. Brunet-Bruneau, H. Amenitsch, P. A. Albouy, C. Sanchez, Chem. Mater. 15 (2003) 4562–4570.
[7] L.-H. Kao, T.-C. Hsu, K.-K. Cheng, J. Colloid Interf. Sci. 341 (2010) 359–365.
[8] D. Grosso, G. J. de A. A. Soler-Illia, F. Babonneau, C. Sanchez, P.-A. Albouy, A. Brunet-Bruneau, A. R. Balkenende, Adv. Mater. 13 (2001) 1085–1090.
[9] W. Choi, A. Termin, M. R. Hoffmann, J. Phys. Chem. 98 (1994) 13669–13679.
[10] R. Asahi, T. Morikawa, T. Ohwaki, K. Aoki, Y. Taga, Science 293 (2001) 269–271.
[11] K. S. W. Sing, D. H. Everett, R. A. W. Haul, L. Moscou, R. A. Pierotti, J. Rouquerol, T. Siemieniwska, Pure Appl. Chem. 57 (1985) 603–619.
[12] A. C. Ferrari, J. Robertson, Phys. Rev. B 64 (2001) 075414.
[13] T. Wu, G. Liu, J. Zhao, H. Hidaka, N. Serpone, J. Phys. Chem. B 102 (1998) 5845–5851.
[14] S. Sakthivel, H. Kisch, Angew. Chem. Int. Ed. 42 (2003) 4908–4911.
[15] Y. J. Chen, G. Y. Jhan, G. L. Cai, C. S. Lin, M. S. Wong, S.-C. Ke, H. H. Lo, C. L. Cheng, J.-J. Shyue, J. Vac. Sci. Technol. A 28 (2010) 779–782.